

# Broken symmetry, excitons, gapless modes and topological excitations in Trilayer Quantum Hall systems

Jinwu Ye

*Department of Physics, The Pennsylvania State University, University Park, PA, 16802*

(December 2, 2024)

We study the interlayer coherent incompressible phase in Trilayer Quantum Hall systems (TLQH) at total filling factor  $\nu_T = 1$  from three approaches: Mutual Composite Fermion (MCF), Composite Boson (CB) and wavefunction approach. Just like in Bilayer Quantum Hall system, CB approach is more superior than MCF approach in studying TLQH. The Hall and Hall drag resistivities are found to be quantized at  $h/e^2$ . Two neutral gapless modes which are left and right moving modes with linear dispersion relations  $v_{l/r} = \omega_{l/r} k$  are identified and the ratio of the two velocities is close to  $\sqrt{3}$ . The novel excitation spectra are classified into two classes: Charge neutral bosonic 2-body bound states and Charge  $\pm 1$  fermionic 3-body bound states. In general, there are two 2-body Kosterlitz-Thouless (KT) transition temperatures and one 3-body KT transition. The Charge  $\pm 1$  3-body fermionic bound states may be the main dissipation source of transport measurements. The broken symmetry in terms of  $SU(3)$  algebra is studied. The structure of excitons and their flowing patterns are given. Limitations and drawbacks of the CB approach are also pointed out.

## I. INTRODUCTION

Quantum Hall Effects (FQHE) in multicomponent systems has attracted a lot of attention since the seminal work by Halperin [1]. These components could be the spins of electrons when the Zeeman coupling is very small or layer indices in multi-layered system. In particular, spin-polarized Bilayer Quantum Hall (BLQH) systems at total filling factor  $\nu_T = 1$  have been under enormous experimental and theoretical investigations over the last decade [2]. When the interlayer separation  $d$  is larger than a critical distance  $d_c/l \sim 1.8$  where  $l$  is the magnetic length, the bilayer system decouples into two separate compressible  $\nu = 1/2$  layers. Earlier experiments exhibited a strong suppression of the tunneling current at low biases [3]. However, when  $d < d_c$ , in the absence of interlayer tunneling, the system undergoes a quantum phase transition into a novel spontaneous interlayer coherent incompressible phase [2]. Recently, at low temperature, with extremely small interlayer tunneling amplitude, Spielman *et al* discovered a very pronounced narrow zero bias peak in this interlayer coherent incompressible state [4]. M. Kellogg *et al* also observed quantized Hall drag resistance at  $h/e^2$  [5]. In very recent counterflow experiments, both the longitudinal and Hall resistances vanish in the low temperature limit [6].

By treating the two layer indices as two pseudo-spin indices, Girvin, Macdonald and collaborators [10,11,2] mapped the bilayer system into a Easy Plane Quantum Ferromagnet (EPQFM) by projecting the Hamiltonian of the BLQH onto the Lowest Landau Level (LLL) and then using subsequent Hartree-Fock (HF) approximation and gradient expansion ( called LLL+HF in the following ). They explored many rich and interesting physical phenomena in this system. The low energy excitations above the ground state is given by an effective 2+1 dimensional XY model. In addition to the Goldstone mode, there

are also 4 flavors of topological defects called " merons " which carry fractional charges  $\pm 1/2$  and also have  $\pm$  vorticity. They have logarithmic divergent self energies and are bound into pairs at low temperature. The lowest energy excitations carry charge  $\pm e$  which are a meron pair with opposite vorticity and the same charge. There is a finite temperature Kosterlitz-Thouless (KT) phase transition at  $T_{KT}$  where bound states of the 4 flavors of merons are broken into free merons. Unfortunately, this transition has not been observed so far. The EPQFM approach is a microscopic one which takes care of LLL projection from the very beginning. However, the charge sector was explicitly projected out, the connection and coupling between the charge sector which displays Fractional Quantum Hall effect and the spin sector which displays interlayer phase coherence was not obvious in this approach.

Just like in SLQH, there are two kinds of Chern-Simon theory approaches. Composite Boson (CB) and Composite Fermion (CF). Using CB approach, the authors in [9–11,2] studied the BLQH. This CB approach focuses on the order parameter in pseudo-spin sector. It can bring out explicitly the broken symmetry in the ground state and associated Goldstone modes. It can also be smoothly connected to  $d \rightarrow 0$  limit which is essentially the same as a single layer unpolarized real spin problem [12]. Using Composite Fermion (CF) theory approach, the authors in [8] also discovered a Neutral Gapless Mode (NGM) with linear dispersion relation  $\omega \sim v k$  and conjectured that there is a finite temperature Kosterlitz-Thouless (KT) phase transition associated with this NGM [8]. There are also many other works along this line of CF approach [13].

In [14], I used both Mutual Composite Fermion (MCF) and CB approaches to study BLQH and made critical comparisons between the two approaches. I identified several serious problems with the MCF approach and

then developed a simple CB approach which can avoid all these problems suffered in the MCF approach. I found the CB approach is more superior to MCF approach in the study of BLQH. Instead of integrating out the gapped charge sector which was done in the previous CB approach [9–11,2], this CB approach has the advantage to treat charged excitations and the collective order parameter fluctuations in the pseudo-spin sector *on the same footing*, therefore can spell out the spin-charge connections explicitly. From this spin-charge connection, we are able to classify all the possible excitations in the BLQH. It may also be applied to study the incoherent disordered insulating side and the quantum phase transitions between different ground states [15]. Using the CB approach, I also studied several interesting phenomena specific to im-balanced BLQH. Just like any Chern-Simon theory, the CB theory in BLQH has its own drawbacks: it is hard to incorporate the LLL projection ( see however [20] ), some parameters can only be taken as phenomenological paramters fitted into the microscopic LLL+HF calculations or experimental data. It is an effective low energy theory, so may not capture some physics at microscopic length scales

In this paper, we use both MCF approach and the CB approach developed in [14] to study Trilayer Quantum Hall (TLQH) systems. We also supplement the two approaches by wavefunction approach. On the theory side, TLQH is interesting, because the three layers play the roles of three flavors. The excitons in BLQH is the pairing of particle in one layer and the hole in the other. This pairing structure in BLQH is similar to the Cooper pairing in BCS superconductors up to a particle-hole transformation. While the excitons in TLQH is not obvious, because so far there is no analog of three flavors superconductors yet. It would be interesting to understand the structures of the excitons and all the possible excitations in TLQH. There are three possible regimes for TLQH. (I) Interlayer coherent regime  $0 < d < d_c/2$  where all the three layers are strongly correlated. (II) Mixed regime  $d_c/2 < d < d_c$ . In this case, layer 2 is strongly coupled to both layer 1 and layer 3, but layer 1 and layer 3 are only weakly coupled, because their distance  $2d$  is larger than the critical distance. (III) Weakly-coupled regime  $d > d_c$  where all the three layers are weakly coupled. In this paper, we focus on regime (I) which is the interlayer coherent regime. On the experimental side, TLQH systems have been fabricated in high mobility electron systems in the experimental group led by Shayegan [17]. The system in the interlayer coherent regime (I) was discussed theoretically in [7,18] in HF approximation, two Goldstone modes are found. Here, we study the model from both MCF and CB approaches and also stress the broken symmetry state in terms of  $SU(3)$  algebra

Consider a tri-layer system with  $N_1, N_2, N_3$  electrons in layer 1 ( the bottom layer ), layer 2 ( the middle layer ) and layer 3 ( the top layer ) respectively with

equal interlayer distance  $d$  between adjacent layers in the presence of magnetic field  $\vec{B} = \nabla \times \vec{A}$ , the Hamiltonian  $H = H_0 + H_{int}$  is

$$H_0 = \int d^2x c_\alpha^\dagger(\vec{x}) \frac{(-i\hbar\vec{\nabla} + \frac{e}{c}\vec{A}(\vec{x}))^2}{2m} c_\alpha(\vec{x})$$

$$H_{int} = \frac{1}{2} \int d^2x d^2x' \delta\rho_\alpha(\vec{x}) V_{\alpha\beta}(\vec{x} - \vec{x}') \delta\rho_\beta(\vec{x}') \quad (1)$$

where electrons have bare mass  $m$  and carry charge  $-e$ ;  $c_\alpha, \delta\rho_\alpha(\vec{x}) = c_\alpha^\dagger(\vec{x})c_\alpha(\vec{x}) - n_\alpha, \alpha = 1, 2, 3$  are electron operators and normal ordered electron densities on the three layers. The intralayer interactions are  $V_{11} = V_{22} = V_{33} = e^2/\epsilon r$ , while interlayer interaction is  $V_{12} = V_{21} = V_{23} = V_{32} = e^2/\epsilon\sqrt{r^2 + d^2}, V_{13} = V_{31} = e^2/\epsilon\sqrt{r^2 + 4d^2}$  where  $\epsilon$  is the dielectric constant.

The rest of the paper is organized as follows. In section II, we discuss MCF approach to TLQH and point out its weakness. In section III, we discuss CB approach and calculate the two spin wave velocities. We also derive a dual action of the CB approach and make critical comparisons between this dual action and the MCF action. We also classify all the possible excitations and discuss possible 2-body and 3-body bound states and associated Kosterlitz-Thouless transitions. We reach conclusions in the final section. At approiate places, we point out the drawbacks of the CB approach compared to microscopic calculations in the LLL performed in a future work [19].

## II. MUTUAL COMPOSITE FERMION APPROACH:

We can extend the single-valued singular gauge transformation (SGT) in [14] to tri-layer system:

$$U = e^{\frac{i}{2} \sum_{\alpha\beta} \int d^2x \int d^2x' U_{\alpha\beta} \rho_\alpha(\vec{x}) \text{arg}(\vec{x} - \vec{x}') \rho_\beta(\vec{x}')} \quad (2)$$

where the  $3 \times 3$  symmetric matrix  $U$  and its inverse is given by:

$$U_t = \begin{pmatrix} 0 & 1 & 1 \\ 1 & 0 & 1 \\ 1 & 1 & 0 \end{pmatrix} \quad U_t^{-1} = \frac{1}{2} \begin{pmatrix} -1 & 1 & 1 \\ 1 & -1 & 1 \\ 1 & 1 & -1 \end{pmatrix} \quad (3)$$

The Hamiltonian Eqn.1 is transformed into:

$$H_0 = \int d^2x \psi_\alpha^\dagger(\vec{x}) \frac{(-i\hbar\vec{\nabla} + \frac{e}{c}\vec{A}(\vec{x}) - \hbar\vec{a}_\alpha(\vec{x}))^2}{2m} \psi_\alpha(\vec{x}) \quad (4)$$

where the transformed fermion  $\psi_\alpha(\vec{x}) = U c_\alpha(\vec{x}) U^{-1}$  is given by:

$$\psi_\alpha(\vec{x}) = e^{\frac{i}{2} \int d^2x' U_{\alpha\beta} [\text{arg}(\vec{x} - \vec{x}') + \text{arg}(\vec{x}' - \vec{x})] \rho_\beta(\vec{x}')} \quad (5)$$

and the three Chern-Simon (CS) gauge fields  $a_\alpha$  in Eqn.4 satisfies:  $\nabla \cdot \vec{a}_\alpha = 0, \nabla \times \vec{a}_\alpha = 2\pi U_{\alpha\beta} \rho_\beta(\vec{x}) = 2\pi [\rho(\vec{x}) -$

$\rho_\alpha(\vec{x})]$  where  $\rho(\vec{x}) = \sum_\alpha \rho_\alpha(\vec{x})$  is the total density of the system.

In the following, we put  $\hbar = c = e = \epsilon = 1$ . At total filling factor  $\nu_T = 1$ ,  $\nabla \times \vec{A} = 2\pi n$  where  $n = n_1 + n_2 + n_3$  is the total average electron density. By absorbing the average values of C-S gauge fields  $\nabla \times \langle \vec{a}_\alpha \rangle = 2\pi(n - n_\alpha)$  into the external gauge potential  $\vec{A}_\alpha^* = \vec{A} - \langle \vec{a}_\alpha \rangle$ , we have:

$$H_0 = \int d^2x \psi_\alpha^\dagger(\vec{x}) \frac{(-i\vec{\nabla} + \vec{A}_\alpha^*(\vec{x}) - \delta\vec{a}_\alpha(\vec{x}))^2}{2m} \psi_\alpha(\vec{x}) \quad (6)$$

where  $\nabla \times \vec{A}_\alpha^* = 2\pi n_\alpha$  and  $\nabla \times \delta\vec{a}_\alpha = 2\pi U_{\alpha\beta} \delta\rho_\beta(\vec{x}) = 2\pi[\delta\rho(\vec{x}) - \delta\rho_\alpha(\vec{x})]$  are the deviations from the corresponding average density.

When  $d < d_c/2$ , the strong intra- and inter-layer interactions renormalize the bare mass into two different effective masses  $m_1^* = m_3^*, m_2^*$  [20]. MCF in each layer feel effective magnetic field  $B_\alpha^* = \nabla \times \vec{A}_\alpha^* = 2\pi n_\alpha$ , therefore fill exactly one MCF Landau level. The energy gaps are simply the cyclotron gaps of the MCF Landau levels  $\omega_{c\alpha}^* = \frac{B_\alpha^*}{m_\alpha^*}$ .

Transport properties: Adding three different source gauge potentials  $\vec{A}_\alpha^s$  to the three layers in Eqn.6, integrating out the MCF  $\psi_\alpha$  first, then the mutual C-S gauge fields, we can calculate the resistivity tensor by Kubo formula. We find that both Hall resistivity and two Hall drag resistivities are  $h/e^2$ . This means if one drives current in one layer, the Hall resistivities in all the three layers are quantized at  $h/e^2$ , while the longitudinal resistivities in all the three layers vanish. This is the hallmark of interlayer coherent quantum hall states.

In the following, we confine to balanced case  $N_1 = N_2 = N_3 = N/3$ , imbalanced case can be discussed along the similar line developed in [14].

Fractional charges: Let's look at the charge of quasi-particles created by MCF field operators  $\psi_\alpha^\dagger(\vec{x})$ . If we insert one electron at one of the layers, say layer 1, from the SGT Eqn.2, we can see this is equivalent to insert one MCF in layer 1, at the same time, insert one flux quantum at layer 2 and another one at layer 3 directly above the position where we inserted the electron. The inserted flux quantum at layer 2 and layer 3 are in the opposite direction to the external magnetic field, therefore promote one MCF in layer 2 and one in layer 3 to the second MCF Landau level in layer 2 and layer 3 respectively. Because inserting one electron leads to three MCFs in each layer, we conclude the charge of each MCF is  $-1/3$ . The above argument gives the correct *total* fractional charges of MCF, but it can not determine the *relative* charge distributions among the three layers. At mean field level, the energies of all the possible relative charge differences are degenerate. The lowest energy configuration can only be determined by fluctuations.

Left- and right-moving gapless modes:  $\delta\rho_\alpha(\vec{x})$  can be expressed in terms of the C-S gauge fields  $\delta\rho_\alpha(\vec{x}) =$

$[U_t^{-1}]_{\alpha\beta} \frac{\delta\vec{a}_\beta}{2\pi}$  where  $U_t^{-1}$  is given in Eqn.3. This constraint can be imposed by Lagrangian multipliers  $a_\alpha^0$  which plays the role of time components of C-S gauge fields. Integrating out MCF  $\psi_1, \psi_2, \psi_3$  to one-loop and carefully expanding the interlayer Coulomb interaction to the necessary order in the long-wavelength limit leads to an effective action for the three gauge fields.

$$\begin{aligned} \mathcal{L} = & \frac{iq}{4\pi} a_c^0 a_c^t + \frac{q}{16\pi} (a_c^t)^2 \\ & + \frac{\epsilon_c}{6} q^2 (a_c^0)^2 + \frac{1}{6} [\epsilon_c \omega^2 + (\chi_c - \frac{d}{3\pi}) q^2] (a_c^t)^2 \\ & + \frac{\epsilon_l}{4} q^2 (a_l^0)^2 + \frac{1}{4} [\epsilon_l \omega^2 + (\chi_l + \frac{d}{\pi}) q^2] (a_l^t)^2 \\ & + \frac{\epsilon_r}{12} q^2 (a_r^0)^2 + \frac{1}{12} [\epsilon_r \omega^2 + (\chi_r + \frac{d}{3\pi}) q^2] (a_r^t)^2 \\ & + \frac{\delta\epsilon}{9} q^2 a_c^0 a_r^0 + \frac{1}{9} [\delta\epsilon \omega^2 + (\delta\chi + \frac{d}{4\pi}) q^2] a_c^t a_r^t + \dots \end{aligned} \quad (7)$$

where  $\vec{a}_s = \vec{a}_1 + \vec{a}_2 + \vec{a}_3$ ,  $\vec{a}_l = \vec{a}_1 - \vec{a}_3$ ,  $\vec{a}_r = \vec{a}_1 + \vec{a}_3 - 2\vec{a}_2$  which stand for center of mass, left moving and right moving modes respectively.  $\epsilon_c = (2\epsilon_1 + \epsilon_2)/3$ ,  $\chi_c = (2\chi_1 + \chi_2)/3$ ,  $\epsilon_l = \epsilon_1$ ,  $\chi_l = \chi_1$ ,  $\epsilon_r = (\epsilon_1 + 2\epsilon_2)/3$ ,  $\chi_r = (\chi_1 + 2\chi_2)/3$ ,  $\delta\epsilon = \epsilon_1 - \epsilon_2$ ,  $\delta\chi = \chi_1 - \chi_2$ . The dielectric constants  $\epsilon_\alpha = \frac{m_\alpha^*}{2\pi B_\alpha^*}$  and the susceptibilities  $\chi_\alpha = \frac{1}{2\pi m_\alpha^*}$  were calculated in single layer system in [21].  $\dots$  are higher gradient terms and  $a_\alpha^t$  is the transverse component of gauge fields in Coulomb gauge  $\nabla \cdot \vec{a}_\alpha = 0$ . The system is invariant under the  $Z_2$  symmetry which exchanges layer 1 and 3, namely  $a_c \rightarrow a_c$ ,  $a_l \rightarrow -a_l$ ,  $a_r \rightarrow a_r$ . This symmetry dictates that only  $a_c a_c, a_c a_r, a_r a_r, a_l a_l$  can appear in the Maxwell terms. The last two terms in Eqn. 7 which is the coupling between  $a_c$  and  $a_r$  can be shown to be irrelevant in the low energy limit.

More intuitive choices are  $a_u = a_1 - a_2$ ,  $a_d = a_2 - a_3$  which is related to  $a_l, a_r$  by  $a_l = a_u + a_d$ ,  $a_r = a_u - a_d$ . But  $a_u$  and  $a_d$  are coupled, the two normal modes are  $a_l, a_r$  instead of  $a_u, a_d$ . As expected, there is a Chern-Simon term for the center of mass gauge field  $\vec{a}_s$ , while there are two Maxwell terms for the left and right moving gauge fields  $\vec{a}_l, \vec{a}_r$  which are gapless. The two gapless modes stand for the relative charge density fluctuations among the three layers. After putting back  $\hbar, c, e, \epsilon$ , we find the two spin-wave velocities in terms of experimentally measurable parameters:

$$\begin{aligned} v_l^2 &= \frac{3(\omega_c^*)^2}{2\pi n} + \left(\frac{2\alpha c}{\epsilon}\right) \left(\frac{d}{l}\right) \frac{\omega_c^*}{\sqrt{2\pi n}} \\ v_r^2 &= \frac{3(\omega_c^*)^2}{2\pi n} \frac{1 + 2\gamma^{-1}}{1 + 2\gamma} + \left(\frac{2\alpha c}{\epsilon}\right) \left(\frac{d}{l}\right) \frac{\omega_c^*}{\sqrt{2\pi n}} \frac{1}{1 + 2\gamma} \end{aligned} \quad (8)$$

where we set  $\omega_c^* = \omega_{c1}^*$  and  $n$  is the total density,  $l$  is the magnetic length,  $\gamma$  is the ratio of the two effective masses  $\gamma = m_2^*/m_1^*$  and  $\alpha \sim 1/137$  is the fine structure constant.

As in BLQH [14], we expect the second term dominates the first, then  $v_l/v_r \sim \sqrt{1 + 2\gamma}$ . namely, the ratio

of the two velocities is determined by the ratio of the two effective masses. If we take the effective masses to be the band mass, then  $v_l/v_r \sim \sqrt{3}$ .

Topological excitations: As discussed in the previous paragraph, the MCF carries charge  $1/3$ , but their relative charge distributions among the three layers are undetermined. They can be characterized by their  $(a_c, a_l, a_r)$  charges  $(\pm 1/3, q_l, q_r)$  with  $q_l, q_r = 0, \pm 1, \dots$ . Exchanging  $a_c$  leads to  $1/r$  interaction between two MCF, while exchanging  $a_l, a_r$  leads to logarithmic interactions which may lead to a 2-body bound state between two MCF with opposite  $(q_l, q_r)$ . The energy of this bound state with length  $L$  is  $\Delta_+ + \Delta_- + q_c^2 \frac{e^2}{L} - (q_{l1}q_{l2} + \frac{q_{r1}q_{r2}}{1+2\gamma}) \hbar \omega_c^* \ln L/l$  where  $\Delta_+, \Delta_-$  are the core energies of QH and QP respectively. There are also possible 3-body bound states of three MCF with  $\sum_i q_{li} = \sum_i q_{ri} = 0$ .

Unfortunately, the gluing conditions (or selection rules) of  $(q_c, q_l, q_r)$  for realizable physical excitations are not clear. This charge  $q_c$  and two spin  $(q_l, q_r)$  connections can only be easily established from CB approach presented in the next section. So we defer the discussion on the classification of all the possible excitations to the next section.

#### Problems with MCF approach:

All the criticisms on MCF approach to BLQH also hold to TLQH. In the following, we list just ones which are the most relevant to this paper.

(a) It is easy to see that the spin wave dispersion in Eqn.8 remains linear  $\omega \sim vk$  even in the  $d \rightarrow 0$  limit. This contradicts with the well established fact that in the  $d \rightarrow 0$  limit, the linear dispersion relation will be replaced by quadratic  $SU(3)$  Ferromagnetic spin-wave dispersion relation  $\omega \sim k^2$  due to the enlarged  $SU(3)$  symmetry at  $d \rightarrow 0$ .

(b) The broken symmetry in the ground state is not obvious without resorting to the  $(111, 111)$  wavefunction Eqn.28. The origin of the gapless mode is not clear.

(c) The physical meaning of  $q_l, q_r$  is not clear. That they have to be integers was put in by hand in an ad hoc way.

(d) The spin-charge connections in  $(q_c, q_l, q_r)$  can not be extracted.

(e) Even in the balanced case, there are two MCF cyclotron gaps  $\hbar \omega_{ca}^*$ ,  $\alpha = 1, 2$  at mean field theory. However, there is only one charge gap in the system. It is not known how to reconcile this discrepancy within MCF approach.

In the following, we will show that the alternative CB approach not only achieve all the results, but also can get rid of all these drawbacks.

### III. COMPOSITE BOSON APPROACH

Composite boson approach was found to be much more effective than the MCF approach in BLQH. We expect

it remains true in TLQH. In this section, we apply CB approach to study TLQH and find that it indeed avoids all the problems suffered in MCF approach listed in the last section. Instead of integrating out the charge degree of freedoms which was done in the previous CB approach, we keep one charge sector and two spin sectors on the same footing and explicitly stress the spin and charge connections. We classify all the possible excitations, bound states and associated KT transitions.

By defining the center of mass, left-moving and right-moving densities as:

$$\begin{aligned}\delta\rho_c &= \delta\rho_1 + \delta\rho_2 + \delta\rho_3 \\ \delta\rho_l &= \delta\rho_1 - \delta\rho_3 \\ \delta\rho_r &= \delta\rho_1 - 2\delta\rho_2 + \delta\rho_3\end{aligned}\quad (9)$$

We can rewrite  $H_{int}$  in Eqn.1 as:

$$\begin{aligned}H_{int} &= \frac{1}{2}\delta\rho_1 U \delta\rho_1 + \frac{1}{2}\delta\rho_2 U \delta\rho_2 + \frac{1}{2}\delta\rho_3 U \delta\rho_3 \\ &+ \delta\rho_1 V \delta\rho_2 + \delta\rho_2 V \delta\rho_3 + \delta\rho_1 W \delta\rho_3 \\ &= \frac{1}{2}\delta\rho_c V_c \delta\rho_c + \frac{1}{2}\delta\rho_l V_l \delta\rho_l + \frac{1}{2}\delta\rho_r V_r \delta\rho_r + \delta\rho_c V_{cr} \delta\rho_r\end{aligned}\quad (10)$$

where  $U = V_{11}$ ,  $V = V_{12}$ ,  $W = V_{13}$  and  $V_c = \frac{U}{3} + \frac{4V}{9} + \frac{2W}{9}$ ,  $V_l = \frac{1}{2}(U - W)$ ,  $V_r = \frac{1}{3}(\frac{U}{2} - \frac{2V}{3} + \frac{w}{6})$ ,  $V_{cr} = -\frac{1}{9}(V - W)$ . The stability of the system dictates  $V_c V_r - V_{cr}^2 > 0$ . In the long wavelength limit  $qd \ll 1$ , we only keep the leading terms:  $V_c = \frac{2\pi}{q}$ ,  $V_l = 2\pi d$ ,  $V_r = \frac{2\pi d}{9}$ ,  $V_{cr} = -\frac{2\pi d}{9}$ .

Performing a singular gauge transformation:

$$\phi_a(\vec{x}) = e^{i \int d^2 x' \arg(\vec{x} - \vec{x}') \rho(\vec{x}')} c_a(\vec{x}) \quad (11)$$

where  $\rho(\vec{x}) = c_1^\dagger(\vec{x})c_1(\vec{x}) + c_2^\dagger(\vec{x})c_2(\vec{x}) + c_3^\dagger(\vec{x})c_3(\vec{x})$  is the total density of the tri-layer system.

After absorbing the external gauge potential  $\vec{A}$  into the Chern-Simon gauge potential  $\vec{a}$ , we can transform the Hamiltonian Eqn.1 into the Lagrangian in the Coulomb gauge:

$$\begin{aligned}\mathcal{L} &= \phi_a^\dagger(\partial_\tau - ia_0)\phi_a + \phi_a^\dagger(\vec{x}) \frac{(-i\hbar \vec{\nabla} + \frac{e}{c} \vec{A}(\vec{x}) - \hbar \vec{a}(\vec{x}))^2}{2m} \phi_a(\vec{x}) \\ &+ ia_0 \bar{\rho} + \frac{1}{2} \int d^2 x' \delta\rho_c(\vec{x}) V_c(\vec{x} - \vec{x}') \delta\rho_c(\vec{x}') \\ &+ \frac{1}{2} \int d^2 x' \delta\rho_l(\vec{x}) V_l(\vec{x} - \vec{x}') \delta\rho_l(\vec{x}') \\ &+ \frac{1}{2} \int d^2 x' \delta\rho_r(\vec{x}) V_r(\vec{x} - \vec{x}') \delta\rho_r(\vec{x}') \\ &+ \int d^2 x' \delta\rho_c(\vec{x}) V_{cr}(\vec{x} - \vec{x}') \delta\rho_r(\vec{x}') - \frac{i}{2\pi} a_0 (\nabla \times \vec{a})\end{aligned}\quad (12)$$

In the Coulomb gauge, integrating out  $a_0$  leads to the constraint:  $\nabla \times \vec{a} = 2\pi(\phi_a^\dagger \phi_a - \bar{\rho})$ .

It can be shown that  $\phi_a(\vec{x})$  satisfies all the boson commutation relations. We write the three bosons in terms of magnitude and phase

$$\phi_a = \sqrt{\bar{\rho}_a + \delta\rho_a} e^{i\theta_a} \quad (13)$$

The boson commutation relations imply that  $[\delta\rho_a(\vec{x}), \phi_b(\vec{x})] = i\hbar\delta_{ab}\delta(\vec{x} - \vec{x}')$ . For simplicity, in this paper, we only consider the balanced case, so we set  $\bar{\rho}_a = \bar{\rho}$ . The imbalanced case can be discussed along similar lines developed in [14].

We define the center of mass, left-moving and right-moving angles which are conjugate angle variables to the three densities defined in Eqn.9

$$\begin{aligned} \theta_c &= \theta_1 + \theta_2 + \theta_3 \\ \theta_l &= \theta_1 - \theta_3 \\ \theta_r &= \theta_1 - 2\theta_2 + \theta_3 \end{aligned} \quad (14)$$

which satisfy the commutation relations  $[\delta\rho_\alpha(\vec{x}), \phi_\beta(\vec{x}')] = A_\alpha i\hbar\delta_{\alpha\beta}\delta(\vec{x} - \vec{x}')$  where  $A = 3, 2, 6$  for  $\alpha = c, l, r$ .

Substituting Eqn.13 into Eqn.12, neglecting the magnitude fluctuations in the spatial gradient term which were shown to be irrelevant in BLQH in [14] and rewriting the spatial gradient term in terms of the three angles in Eqn.14, we find:

$$\begin{aligned} \mathcal{L} = & i\delta\rho_c\left(\frac{1}{3}\partial_\tau\theta_c - a_0\right) + \frac{\bar{\rho}}{2m}\left[\frac{1}{3}\nabla\theta_c - \vec{a}\right]^2 + \frac{1}{2}\delta\rho_cV_c(\vec{q})\delta\rho_c \\ & + \frac{i}{2}\delta\rho_l\partial_\tau\theta_l + \frac{\bar{\rho}}{12m}(\nabla\theta_l)^2 + \frac{1}{2}\delta\rho_lV_l(\vec{q})\delta\rho_l \\ & + \frac{i}{6}\delta\rho_r\partial_\tau\theta_r + \frac{\bar{\rho}}{36m}(\nabla\theta_r)^2 + \frac{1}{2}\delta\rho_rV_r(\vec{q})\delta\rho_r \\ & + \delta\rho_cV_{cr}(\vec{q})\delta\rho_r - \frac{i}{2\pi}a_0(\nabla \times \vec{a}) \end{aligned} \quad (15)$$

In the balanced case, the symmetry is  $U(1)_c \times U(1)_l \times U(1)_r \times Z_2$  where the first is a local gauge symmetry, the second and the third are global symmetries and the global  $Z_2$  symmetry is the exchange symmetry between layer 1 and layer 3.

### (1) Spin-wave excitation:

At temperatures much lower than the vortex excitation energy, we can neglect vortex configurations in Eqn.15 and only consider the low energy spin-wave excitation. The charge sector ( $\theta_c$  mode) and the two spin sectors ( $\theta_l, \theta_r$  modes) are essentially decoupled. It can be shown that the second to the last term  $\delta\rho_cV_{cr}(\vec{q})\delta\rho_r$  in Eqn.15 which is the coupling between the charge sector and right-moving sector is irrelevant in the long wave-length limit. Therefore, the charge sector is essentially the same as the CSGL action in BLQH. Using the constraint  $a_t = \frac{2\pi\delta\rho_c}{q}$ , neglecting vortex excitations in the ground state and integrating out  $\delta\rho_c$  leads to the effective action of  $\theta_+$ :

$$\mathcal{L}_c = \frac{1}{2} \times \left(\frac{1}{3}\right)^2 \theta_c(-\vec{q}, -\omega) \left[ \frac{\omega^2 + \omega_q^2}{V_c(q) + \frac{4\pi^2\bar{\rho}}{m}\frac{1}{q^2}} \right] \theta_c(\vec{q}, \omega) \quad (16)$$

where  $\omega_q^2 = \omega_c^2 + \frac{\bar{\rho}}{m}q^2V_c(q)$  and  $\omega_c = \frac{2\pi\bar{\rho}}{m}$  is the cyclotron frequency.

From Eqn.16, we can find the equal time correlator of  $\theta_c$ :

$$\begin{aligned} <\theta_c(-\vec{q})\theta_c(\vec{q})> &= \int_{-\infty}^{\infty} \frac{d\omega}{2\pi} <\theta_+(-\vec{q}, -\omega)\theta_+(\vec{q}, \omega)> \\ &= 3 \times \frac{2\pi}{q^2} + O\left(\frac{1}{q}\right) \end{aligned} \quad (17)$$

which leads to the algebraic order:

$$<e^{i(\theta_c(\vec{x})-\theta_c(\vec{y}))}> = \frac{1}{|x - y|^3} \quad (18)$$

We could define  $\tilde{\theta}_c = (\theta_1 + \theta_2 + \theta_3)/3 = \theta_c/3$ , then the exponent will be 1/3. But when we consider topological vortex excitations, then  $e^{i\tilde{\theta}_c}$  may not be single valued. Therefore,  $\theta_c$  is more fundamental than  $\tilde{\theta}_c$ .

While in the spin sector, there are two neutral gapless modes: left-moving mode and right-moving mode. Integrating out  $\delta\rho_l$  leads to

$$\mathcal{L}_l = \frac{1}{2V_l(\vec{q})} \left( \frac{1}{2}\partial_\tau\theta_l \right)^2 + \frac{\bar{\rho}}{12m}(\nabla\theta_l)^2 \quad (19)$$

where the dispersion relation of spin wave can be extracted:

$$\omega^2 = \left[ \frac{2\bar{\rho}}{3m}V_l(\vec{q}) \right] q^2 = v_l^2 q^2 \quad (20)$$

In the long wave-length limit  $qd \ll 1$ , the bare spin wave velocity is:

$$v_l^2 = \frac{\bar{\rho}}{m} \frac{4\pi e^2}{3\epsilon} d = \frac{2e^2}{3m\epsilon} \sqrt{2\pi\bar{\rho}} \left( \frac{d}{l} \right) \quad (21)$$

Integrating out  $\delta\rho_r$  leads to

$$\mathcal{L}_r = \frac{1}{2V_r(\vec{q})} \left( \frac{1}{6}\partial_\tau\theta_r \right)^2 + \frac{\bar{\rho}}{36m}(\nabla\theta_r)^2 \quad (22)$$

where the dispersion relation of spin wave can be extracted:

$$\omega^2 = \left[ \frac{2\bar{\rho}}{m}V_r(\vec{q}) \right] q^2 = v_r^2 q^2 \quad (23)$$

In the long wave-length limit  $qd \ll 1$ , the bare spin wave velocity is:

$$v_r^2 = \frac{\bar{\rho}}{m} \frac{4\pi e^2}{9\epsilon} d = v_l^2/3 \quad (24)$$

Both spin wave velocities should increase as the square root of the separation  $d$  when  $d < d_c/2$ , their ratio  $v_l/v_r \sim \sqrt{3}$ . At  $d = 0$ ,  $v_l = v_r = 0$ . This is expected, because at  $d = 0$  the  $U(1)_l \times U(1)_r \times Z_2$  symmetry is enlarged to  $SU(3)_G$ , the spin wave of  $SU(3)$  isotropic ferromagnet  $\omega \sim k^2$ .

It should be pointed out that the above results are achieved in the CB theory. Just like in BLQH in [14],

some parameters in the CB theory need to be calculated by the microscopic LLL+ HF approach. Although there are no detailed microscopic calculations in TLQH yet except the preliminary work in [7,18], from the insights gained in BLQH, we can still see the drawbacks of the CS approach in TLQH: it is hard to incorporate the LLL projection in this approach, for example, the two spin stiffnesses for the left and right-moving sectors in Eqn.15 should be completely determined by the Coulomb interactions instead of being dependent of the band mass. However, the ratio of the two velocities in Eqn.24 is independent of the band mass, if this ratio remains correct in the microscopic LLL+HF need to be checked [19]. Just like in BLQH, we can simply take  $\rho_l, V_l$  and  $\rho_r, V_r$  in Eqn.15 as phenomenological parameters to be fitted into microscopic calculations or experimental data.

We have also treated the coupling term between the charge and right-moving sector  $\delta\rho_c V_{cr}(\vec{q})\delta\rho_r$  in Eqn.15 exactly and found that in the  $\vec{q}, \omega \rightarrow 0$  limit, the mixed propagator takes the form:

$$\langle \theta_c(-\vec{q}, -\omega) \theta_r(\vec{q}, \omega) \rangle = \frac{\frac{9}{2}(\frac{m}{\pi\rho})^2 V_{cr} \omega^2}{\omega^2 + v_r^2 q^2} \sim \omega^2 \langle \theta_r \theta_r \rangle \quad (25)$$

which is dictated by  $\langle \theta_r \theta_r \rangle$  instead of  $\langle \theta_c \theta_c \rangle$ . Because of the  $\omega^2$  prefactor, we can ignore  $\langle \theta_c \theta_r \rangle$  in the low energy limit.

We also found that Eqns.16, 17, 18 and Eqns.22,23,24 remain true in the long-wavelength and low energy limit, therefore confirm that  $\delta\rho_c V_{cr}(\vec{q})\delta\rho_r$  is indeed irrelevant in the limit.

Just like in BLQH discussed in [14], we can perform a duality transformation on Eqn.15 to obtain a dual action in terms of three vortex currents  $J_\mu^{v;c,l,r} = \frac{1}{2\pi} \epsilon_{\mu\nu\lambda} \partial_\nu \partial_\lambda \theta_{c,l,r}$  and three dual gauge fields  $b_\mu^c, b_\mu^l, b_\mu^r$ :

$$\begin{aligned} \mathcal{L}_d = & -i\pi b_\mu^c \epsilon_{\mu\nu\lambda} \partial_\nu b_\lambda^c - iA_{s\mu}^c \epsilon_{\mu\nu\lambda} \partial_\nu b_\lambda^c + i\frac{2\pi}{3} b_\mu^c J_\mu^v \\ & + \frac{m}{2\bar{\rho}f} (\partial_\alpha b_0^c - \partial_0 b_\alpha^c)^2 + \frac{1}{2} (\nabla \times \vec{b}^c) V_c(\vec{q}) (\nabla \times \vec{b}^c) \\ & - iA_{s\mu}^l \epsilon_{\mu\nu\lambda} \partial_\nu b_\lambda^l + i\pi b_\mu^l J_\mu^v \\ & + \frac{3m}{4\bar{\rho}} (\partial_\alpha b_0^l - \partial_0 b_\alpha^l)^2 + \frac{1}{2} (\nabla \times \vec{b}^l) V_l(\vec{q}) (\nabla \times \vec{b}^l) \\ & - iA_{s\mu}^r \epsilon_{\mu\nu\lambda} \partial_\nu b_\lambda^r + i\frac{\pi}{3} b_\mu^r J_\mu^v \\ & + \frac{m}{4\bar{\rho}} (\partial_\alpha b_0^r - \partial_0 b_\alpha^r)^2 + \frac{1}{2} (\nabla \times \vec{b}^r) V_r(\vec{q}) (\nabla \times \vec{b}^r) \\ & + (\nabla \times \vec{b}^c) V_{cr}(\vec{q}) (\nabla \times \vec{b}^r) \end{aligned} \quad (26)$$

where the three source gauge fields are  $A_{s\mu}^c = A_{1s\mu} + A_{2s\mu} + A_{3s\mu}$ ,  $A_{s\mu}^l = A_{1s\mu} - A_{3s\mu}$ ,  $A_{s\mu}^r = A_{1s\mu} - 2A_{2s\mu} + A_{3s\mu}$ .

We can compare this dual action derived from CB approach with Eqn.7 derived in MCF approach. Just like

in BLQH, the three topological vortex currents are missing in Eqn.7, while  $\chi_c, \chi_l, \chi_r, \delta\chi$  terms are extra spurious terms which break  $SU(3)$  symmetry even in the  $d \rightarrow 0$  limit. If we drop all the  $\chi$  terms, use bare mass and add the three vortex currents terms in Eqn.7, the resulting effective action will be identical to the dual action Eqn.26. Neglecting the vortex currents, we can identify the two spin wave velocities easily from the dual action which are the same as found previously from Eqn.15. It is also easy to show that the last term in Eqn.26 which is the coupling between the charge and right-moving sector is irrelevant in the low energy limit. We conclude that Eqns.15 and its dual action Eqn. 26 are the correct and complete effective actions.

## (2) Topological excitations:

Any topological excitations are characterized by three winding numbers  $\Delta\theta_1 = 2\pi m_1, \Delta\theta_2 = 2\pi m_2, \Delta\theta_3 = 2\pi m_3$ , or equivalently,  $\Delta\theta_c = 2\pi(m_1 + m_2 + m_3) = 2\pi m_c, \Delta\theta_l = 2\pi(m_1 - m_3) = 2\pi m_l, \Delta\theta_r = 2\pi(m_1 - 2m_2 + m_3) = 2\pi m_r$ . It is important to stress that the three fundamental angles are  $\theta_1, \theta_2, \theta_3$  instead of  $\theta_c, \theta_l, \theta_r$ . Therefore,  $m_1, m_2, m_3$  are three independent integers, while  $m_c, m_l, m_r$  are not.

There are following 6 kinds of fundamental topological excitations:  $\Delta\phi_1 = \pm 2\pi$  or  $\Delta\phi_2 = \pm 2\pi$  or  $\Delta\phi_3 = \pm 2\pi$ , namely  $(m_1, m_2, m_3) = (\pm 1, 0, 0), (0, \pm 1, 0), (0, 0, \pm 1)$ . They correspond to inserting one flux quantum in layer 1 or 2 or 3 in the same or opposite direction as the external magnetic field. Let's classify the topological excitations in terms of  $(q, m_l, m_r)$  where  $q$  is the fractional charge of the topological excitations in the following table.

	$(\pm 1, 0, 0)$	$(0, \pm 1, 0)$	$(0, 0, \pm 1)$
$m_c$	$\pm 1$	$\pm 1$	$\pm 1$
$m_l$	$\pm 1$	0	$\mp 1$
$m_r$	$\pm 1$	$\mp 2$	$\pm 1$
$q$	$\pm 1/3$	$\pm 1/3$	$\pm 1/3$

Table 1: The fractional charge in balanced TLQH

The fractional charges in the table were determined from the constraint  $\nabla \times \vec{a} = 2\pi\delta\rho_c$  and the finiteness of the energy in the charge sector:

$$q = \frac{1}{2\pi} \oint \vec{a} \cdot d\vec{l} = \frac{1}{2\pi} \times \frac{1}{3} \oint \nabla\theta_c \cdot d\vec{l} = \frac{1}{3} m_c \quad (27)$$

There are the following two possible bound states:

(1) Three Charge neutral two-body bound states:

- Layer 1:  $(\pm 1/3, \pm 1, \pm 1)$  with energy  $E_1 = E_{c+} + E_{c-} - \frac{e^2}{9R} + 2\pi(\rho_{sl} + \rho_{sr}) \ln \frac{R}{R_c}$  when  $R \gg R_c \gg l$ .
- Layer 2:  $(\pm 1/3, 0, \mp 2)$  with energy  $E_2 = E_{c+} + E_{c-} - \frac{e^2}{9R} + 2\pi(4\rho_{sr}) \ln \frac{R}{R_c}$ .
- Layer 3:  $(\pm 1/3, \mp 1, \pm 1)$  with energy  $E_3 = E_1$  which is dictated by  $Z_2$  symmetry.

The corresponding 2-body Kosterlize-Thouless (KT) transitions are  $k_B T_{KT1}^{2b} = k_B T_{KT3}^{2b} = \frac{\pi}{2}(\rho_{sl} + \rho_{sr})$  which is dictated by  $Z_2$  symmetry and  $k_B T_{KT2}^{2b} = 2\pi\rho_{sr}$  above which the QP and QH pairs are liberated into free ones. If setting  $\rho_{sl} = 3\rho_{sr}$ , then there is only one 2-body KT temperature  $k_B T_{KT}^{2b} = 2\pi\rho_{sr} = \frac{\pi\bar{\rho}}{9m}$ . As explained previously, microscopic calculations in the LLL [19] are needed to estimate the two spin stiffnesses  $\rho_{sl}$  and  $\rho_{sr}$ . In general, there should be two 2-body KT transition temperatures  $k_B T_{KT1}^{2b} = k_B T_{KT3}^{2b} \neq k_B T_{KT2}^{2b}$ . The spin wave excitations will turn into these Charge neutral two-body bound states at large wavevector ( or short distance ). The two-body bound state behaves as a boson.

(1) Two Charge  $\pm 1$  three-body bound states:

The three-body bound states consists of three quasi-particles  $(\pm 1/3, \pm 1, \pm 1), (\pm 1/3, 0, \mp 2), (\pm 1/3, \mp 1, \pm 1)$  located at the three corners of a triangle ( Fig.1 ).

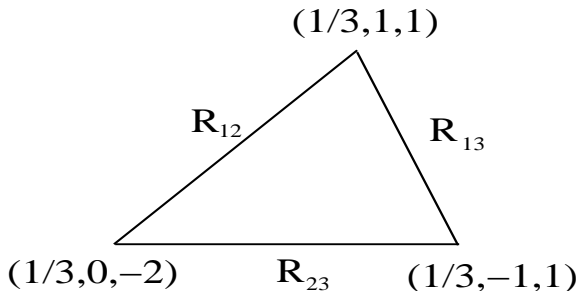


**Fig 1:** The lowest energy charged excitation is a three-body bound state of three  $\pm 1/3$  charged quasi-particles sitting on the three corners of a triangle with  $R_{12} = R_{23}$  dictated by the  $Z_2$  symmetry. The three quantum numbers  $(q, m_l, m_r)$  are enclosed in the paraenthesis

Its energy  $E_{3b} = 3E_{c\pm} + \frac{e^2}{9}(\frac{1}{R_{12}} + \frac{1}{R_{23}} + \frac{1}{R_{13}}) + 2\pi[2\rho_{sr} \ln \frac{R_{12}}{R_c} + (\rho_{sl} - \rho_{sr}) \ln \frac{R_{13}}{R_c} + 2\rho_{sr} \ln \frac{R_{23}}{R_c}]$  when  $R \gg R_c \gg l$ . Minimizing  $E_{3b}$  with respect to  $R_{12}, R_{13}, R_{23}$  leads to two optimal separations:  $R_{o12} = R_{o23} = \frac{e^2}{36\pi\rho_{sr}}$  which is dictated by the  $Z_2$  symmetry and  $R_{o13} = \frac{e^2}{18\pi(\rho_{sl} - \rho_{sr})}$ . If setting  $\rho_{sl} = 3\rho_{sr}$ , then the three quasi-particles are located on the corners of a isosceles with length  $R_o = \frac{e^2}{36\pi\rho_{sr}}$ , the corresponding 3-body Kosterlize-Thouless (KT) transition is the same as the two-body bound state  $k_B T_{KT}^{3b} = k_B T_{KT}^{2b} = 2\pi\rho_{sr} = \frac{\pi\bar{\rho}}{9m}$ . These charged excitations behave as fermions and are the main sources of dissipations in transport experiments. In general,  $T_{KT}^{3b}$  should be different from the two 2-body KT transition temperatures. Again, microscopic calculations of the two spin stiffnesses  $\rho_{sl}$  and  $\rho_{sr}$  in the LLL [19] are needed to determine the three KT transition temperatures.

Let's look at the interesting possibility of deconfined ( or free )  $1/2$  charged excitations. Because any excitations with non-vanishing  $m_l$  or  $m_r$  will be confined, so any deconfined excitations must have  $m_l = m_r = 0$  which

implies  $m_1 = m_2 = m_3 = m$  and  $m_c = 3m$ . Eqn.27 implies the charge  $q = \frac{1}{3}m_c = m$  must be an integer. This proof rigorously rules out the possibility of the existence of deconfined fractional charges. We conclude that *any deconfined charge must be an integral charge*.  $m = 1$  corresponds to inserting one flux quantum through all the three layers which is conventional charge 1 excitation. Splitting the whole flux quantum into three fluxes penetrating the three layers at three different positions will turn into the three-body bound state with the same charge shown in Fig.1. It is still not known if the energy of this conventional charge 1 excitation is lower than the three body bound state.

#### IV. BROKEN SYMMETRY

The broken symmetry and associated Goldstone modes can be easily seen from wavefunction approach. In the first quantization, in the  $d \rightarrow 0$  limit, the ground state trial wavefunction is the  $(111, 111)$  state:

$$\Psi_{111,111} = \prod_{i=1}^{N_1} \prod_{j=1}^{N_2} (u_i - v_j) \prod_{i=1}^{N_1} \prod_{j=1}^{N_3} (u_i - w_j) \prod_{i=1}^{N_2} \prod_{j=1}^{N_3} (v_i - w_j) \times \prod_{i < j}^{N_1} (u_i - u_j) \prod_{i < j}^{N_2} (v_i - v_j) \prod_{i < j}^{N_3} (w_i - w_j) \quad (28)$$

where  $u, v, w$  are the coordinates in layer 1, 2 and 3 respectively.

In the second quantization, a trial wavefunction was written in [18]:

$$|\Psi\rangle = \prod_{m=0}^{M-1} \frac{1}{\sqrt{3}} (e^{i\theta_u} C_{m,1}^\dagger + C_{m,2}^\dagger + e^{i\theta_d} C_{m,3}^\dagger) |0\rangle = \prod_{m=0}^{M-1} \frac{1}{\sqrt{3}} (1 + e^{i\theta_u} C_{m,1}^\dagger C_{m,2} + e^{i\theta_d} C_{m,3}^\dagger C_{m,2}) \times \prod_{m=0}^{M-1} C_{m,2}^\dagger |0\rangle \quad (29)$$

where  $\theta_u = \theta_1 - \theta_2, \theta_d = \theta_3 - \theta_2$  and  $M = N$  is the angular momentum quantum number corresponding to the edge. We can interpret  $\theta_u$  mode in Eqn.29 as a "up" pairing between an electron in layer 1 and a hole in layer 2 which leads to a  $\theta_u$  molecule, similarly,  $\theta_d$  mode as a "down" pairing between an electron in layer 3 and a hole in layer 2 which leads to a  $\theta_d$  molecule ( Fig. 2 ).

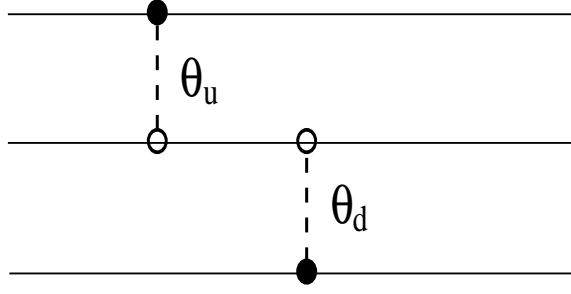


**Fig 2:** Two pairing modes of TLQH. Solid dots are electrons, open dots are holes.

Note that when  $\theta_u = \theta_d = 0$ ,  $|\Psi\rangle$  is the ground state  $|G\rangle$ , it can be shown [16] that its projection on  $(N_1, N_2, N_3)$  sector is  $(111, 111)$  wavefunction in Eqn.28. Note that Eqn.28 is correct only in  $d \rightarrow 0$  limit where the symmetry is enlarged to  $SU(3)$ . In the  $SU(3)$  symmetric case, the pairing between any two layers of the three layers is equally likely. However, at any finite  $d$ , Eqn.28 and Eqn.29 may even not be qualitatively correct [16], because the  $SU(3)$  symmetry is reduced to  $U(1) \times U(1) \times U(1) \times Z_2$  symmetry ( where the three  $U(1)$  symmetry correspond to  $c_\alpha(\vec{x}) \rightarrow e^{i\theta_\alpha} c_\alpha(\vec{x})$ ,  $\alpha = 1, 2, 3$ ,  $c_1 \leftrightarrow c_3$  ) The pairings between any two layers out of the three layers are not equivalent any more. The two lowest energy pairing modes are shown in Fig. 2.

$SU(3)$  has 8 generators which can be written in terms of  $c_\alpha$ :

$$\begin{aligned} S_l(\vec{x}) &= c_1^\dagger(\vec{x})c_1(\vec{x}) - c_3^\dagger(\vec{x})c_3(\vec{x}) \\ S_r(\vec{x}) &= c_1^\dagger(\vec{x})c_1(\vec{x}) + c_3^\dagger(\vec{x})c_3(\vec{x}) - 2c_2^\dagger(\vec{x})c_2(\vec{x}) \\ S_{12}(\vec{x}) &= c_1^\dagger(\vec{x})c_2(\vec{x}), \quad S_{21}(\vec{x}) = S_{12}^\dagger(\vec{x}) = c_2^\dagger(\vec{x})c_1(\vec{x}) \\ S_{23}(\vec{x}) &= c_2^\dagger(\vec{x})c_3(\vec{x}), \quad S_{32}(\vec{x}) = S_{23}^\dagger(\vec{x}) = c_3^\dagger(\vec{x})c_2(\vec{x}) \\ S_{13}(\vec{x}) &= c_1^\dagger(\vec{x})c_3(\vec{x}), \quad S_{31}(\vec{x}) = S_{13}^\dagger(\vec{x}) = c_3^\dagger(\vec{x})c_1(\vec{x}) \end{aligned} \quad (30)$$

where  $S_l, S_r$  are the two ( left and right ) generators in Cartan subalgebra ( Note that the algebra is *not*  $SU(2)$  in spin  $j = 1$  representation which is also 3 dimensional as used in [7] ). In the balanced case  $N_1 = N_2 = N_3 = N/3$ , we have  $\langle S_l \rangle = \langle S_r \rangle = 0$ . The ground state in Eqn.28 *breaks* two of the three  $U(1)$  symmetries, therefore there are two Goldstone modes in the corresponding two order parameters  $\langle S_{12} \rangle = \frac{N}{3}e^{i\theta_u}$ ,  $\langle S_{23} \rangle = \frac{N}{3}e^{-i\theta_d}$ . The two decoupled XY model in terms of  $\theta_l = \theta_u - \theta_d = \theta_1 - \theta_3$ ,  $\theta_r = \theta_u + \theta_d = \theta_1 - 2\theta_2 + \theta_3$  are described by Eqn.15. When  $\theta_u$  molecule and  $\theta_d$  molecule in Fig.2 move in the opposite direction, the currents in layer 2 cancel each other, it leads to the left-moving superfluid channel  $\theta_l$  ( Fig. 3a ). While when  $\theta_u$  molecule and  $\theta_d$  molecule move in the same direction, the currents in layer 2 add and flow in the opposite direction to the currents in layer 1 and layer 3, it leads to the right-moving superfluid channel  $\theta_r$  ( Fig. 3b ). In BLQH, there is only one superfluid channel which is the counter-flow channel [6]. In TLQH, there are two superfluid channels which are left-moving and right-moving channels, the left-moving channel corresponds to the counter-flow channel ( Fig. 3 ). Obviously, it is easier to perform transport experiments in the counter-flow channel than in the right-moving channel.

and right-moving channels, the left-moving channel corresponds to the counter-flow channel. Obviously, it is easier to perform transport experiments in the counter-flow channel than in the right-moving channel.

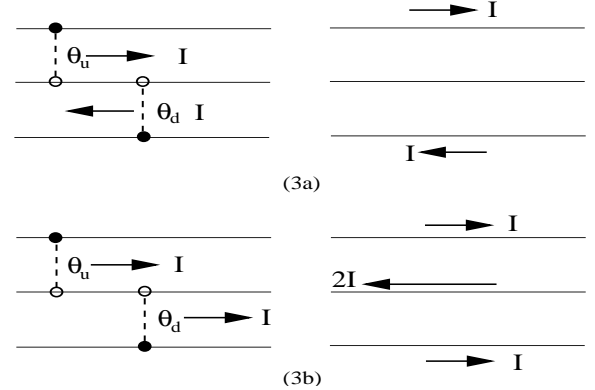


**Fig 3:** (3a) Left-moving superfluid channel which is the counter-flow channel (3b) Right-moving superfluid channel

## V. CONCLUSIONS:

In this paper, we study the interlayer coherent incompressible phase in Trilayer Quantum Hall systems at total filling factor  $\nu_T = 1$  from three approaches: MCF, CB and wavefunction approach. Just like in TLQH, CB approach is more superior than MCF approach. The Hall and Hall drag resistivities are found to be quantized at  $h/e^2$ . Two neutral gapless modes which are left and right moving modes with linear dispersion relations  $v_{l/r} = \omega_{l/r}k$  are identified and the ratio of the two velocities is close to  $\sqrt{3}$ . The novel excitation spectra are classified into two classes: (1) Charge neutral bosonic two-body bound states. (3) Charge  $\pm 1$  fermionic three-body bound states. In general, there are two 2-body KT transition temperatures and one 3-body KT transition temperature. Microscopic calculations in the LLL [19] are needed to determine the three KT transition temperatures. The Charge  $\pm 1$  three-body bound states shown in Fig. 1 may be the main dissipation source of the interlayer tunneling. The broken symmetry in terms of  $SU(3)$  algebra is studied. The effective action of the two associated Goldstone modes are derived. The novel excitonic structure in TLQH was shown in Fig. 2. In BLQH, there is only one superfluid channel which is the counter-flow channel [6]. In TLQH, there are two superfluid channels which are left-moving and right-moving channels, the left-moving channel corresponds to the counter-flow channel ( Fig. 3 ). Obviously, it is easier to perform transport experiments in the counter-flow channel than in the right-moving channel.

We expect that the effective action and the qualitative physical pictures of TLQH achieved from CB approach in

this paper are correct. However, the parameters in the effective action need to be calculated from microscopic calculations in the LLL [19]. It is interesting to see if the ratio  $v_l/v_r \sim \sqrt{3}$  still holds in the microscopic calculations.

I thank J. K. Jain for helpful discussions.

---

- [7] H. Fertig, Phys. Rev. B 40, 1087 (1989).
- [8] X. G. Wen and A. Zee, Phys. Rev. Lett. 69, 1811 (1992).
- [9] Z. F. Ezawa and A. Iwazaki, Phys. Rev. B. 48, 15189 (1993).
- [10] Kun Yang *et al*, Phys. Rev. Lett. 72, 732 (1994).
- [11] K. Moon *et al*, Phys. Rev. B 51, 5138 (1995).
- [12] S. L. Sondhi *et al*, Phys. Rev. B 47, 16419 (1993).
- [13] A. López and E. Fradkin, Phys. Rev. B 51, 4347 (1995), *ibid*, 63, 085306, 2001; V. W. Scarola and J. K. Jain, Phys. Rev. B 64, 085313 (2001); Yong Baek Kim *et al*, cond-mat/0011459; M. Y. Veillette; L. Balents and M. P. A. Fisher, Phys. Rev. B. 66, 155401 (2002).
- [14] Jinwu Ye, cond-mat/0310512
- [15] Jinwu Ye, cond-mat/0407088
- [16] Jinwu Ye and Gun Sang Jeon, cond-mat/0407258.
- [17] J. Jo, Y. W. Suen, L. W. Engel, M. B. Santos, and M. Shayegan, Phys. Rev. B 46, 9776-9779 (1992); T. S. Lay, X. Ying, and M. Shayegan, Phys. Rev. B 52, R5511-5514 (1995).
- [18] C.B. Hanna and A.H. MacDonald, Phys. Rev. B 53 (23): 15981 (1996).
- [19] Jinwu Ye, unpublished.
- [20] See the review by G. Murthy and R. Shankar, Rev. of Mod. Phys. 75, 1101, 2003.
- [21] A. Lopez and E. Fradkin, Phys. Rev. B. 44, 5246 (1991).
- [22] Jinwu Ye and S. Sachdev, Phys. Rev. Lett. 80, 5409 (1998); Jinwu Ye, Phys. Rev. B60, 8290 (1999).